

# Comparative equilibrium and structural studies of new pentamethylcyclopentadienyl rhodium complexes bearing (O,N) donor bidentate ligands

Orsolya Dömötör <sup>\$a,b</sup>, Carmen M. Hackl <sup>\$c</sup>, Krisztina Bali <sup>a</sup>, Alexander Roller <sup>c</sup>, Michaela Hejl <sup>c</sup>, Michael A. Jakupec <sup>c,d</sup>, Bernhard K. Keppler <sup>c,d</sup>, Wolfgang Kandioller <sup>c,d</sup>, and Éva A. Enyedy <sup>\*a</sup>

a Department of Inorganic and Analytical Chemistry, University of Szeged, Dóm tér 7, H-6720 Szeged, Hungary, E-mail: [enyedy@chem.u-szeged.hu](mailto:enyedy@chem.u-szeged.hu)

b MTA-SZTE Bioinorganic Chemistry Research Group, University of Szeged, Dóm tér 7, H-6720 Szeged, Hungary

c Institute of Inorganic Chemistry, Faculty of Chemistry, University of Vienna, Waehringer Str. 42, A-1090 Vienna, Austria

d Research Platform Translational Cancer Therapy Research, University of Vienna, Waehringer Str. 42, A-1090 Vienna, Austria

\$ These authors contributed equally to this work.

**Keywords:** Stability Constants • Solid-state Structure • Speciation • Half-sandwich rhodium complexes

\* Corresponding Author

E-mail address: [enyedy@chem.u-szeged.hu](mailto:enyedy@chem.u-szeged.hu) (É.A. Enyedy).

## Abstract

Complex formation processes of the (O,N) donor ligands 6-methylpicolinic acid (6-Mepic), quinoline-2-carboxylic acid (2-QA) and 3-isoquinolinecarboxylic acid (3-iQA) with the organometallic moiety ( $\eta^5$ -pentamethylcyclopentadienyl)rhodium(III) (RhCp\*) were studied in aqueous solution by the combined use of pH-potentiometry,  $^1\text{H}$  NMR spectroscopy and UV-Vis spectrophotometry. The solid phase structures of the [RhCp\*(L)Cl] complexes bearing 6-Mepic and 2-QA were characterized by single-crystal X-ray diffraction analysis. Studies revealed the exclusive formation of mono complexes of the form [RhCp\*(L)(H<sub>2</sub>O)]<sup>+</sup> (L = deprotonated form of the ligands) and [RhCp\*(L)(OH)]. The positively charged aqua species predominate at physiological pH even in the micromolar concentration range. The H<sub>2</sub>O/Cl<sup>-</sup> co-ligand exchange constants showed that all complexes preferably retain the chlorido ligand at the third coordination site at chloride ion concentrations present in the serum. In addition *in vitro* cytotoxicity of these [RhCp\*(L)Cl] complexes was evaluated in three human cancer cell lines (A549, SW480 and CH1/PA-1) where they showed minor cytotoxic potency.

## Introduction

The field of modern metal-based anticancer drug research was initiated in the late 1960s by the discovery of cisplatin, which is still one of the leading agents in clinical use to treat cancer. The application of cisplatin is often limited by the appearance of side-effects and intrinsic or acquired resistance phenomena [1-3]. In this context, other metals of the platinum group were chosen as a core for similar complexes, intended to convey desirable pharmacological properties. In the early stages, research concentrated on Ru(III) complexes, but later a wider range of metals attracted notice in the development of new anticancer compounds. Prominent representatives of this compound class are KP1019 (indazolium *trans*-[tetrachloridobis(1H-indazole)ruthenate(III)]) [4] as well as its sodium salt IT-139 (NKP-1339) [5] and NAMI-A (imidazolium *trans*-[tetrachlorido(1H-imidazole)(dimethylsulfoxide)ruthenate(III)]) [6], all of which have been characterized in a variety of studies especially with regard to their growth inhibitory effects on cancer cells. IT-139 was selected as lead candidate for further clinical development due to its remarkable *in vivo* activity accompanied by low general toxicity as demonstrated in a phase I/IIa clinical study [5]. Investigations were undertaken to elucidate the mechanism of action of this Ru(III) complex, resulting in the so-called “activation by reduction” hypothesis which indicates that the complex with its metal center in the reduced form accounts for the activity of the

compound. Therefore, half-sandwich Ru(II)- as well as Os(II)-arene complexes are extensively being investigated, and some of them are able to circumvent resistances of cancer cells due to novel mechanisms of action by addressing different targets within the cell [7,8].

To extend the scope of possible organometallic compounds with anticancer properties, Rh(III)-based complexes have been developed. Rh(III)-cyclopentadienyl complexes are isoelectric with Ru(II)-arene complexes and have some chemically attractive properties such as increased aqueous solubility and faster ligand exchange kinetics [9,10]. Recently more and more studies have focused on their antitumor activity [9,11-15]. Among the first reports dealing with the anticancer properties of Rh(III) compounds were those investigating the salt  $\text{RhCl}_3$  and its simple complexes, such as *mer*- $[\text{RhCl}_3(\text{NH}_3)_3]$  [16,17]. Promising antiproliferative activities of organometallic Rh(III) complexes based on (N,N) donating polypyridyl ligands, with  $\text{IC}_{50}$  values in the low micromolar concentration range, have been reported by Sheldrick and co-workers [18-21]. Another very interesting concept involving dirhodium(II,II) complexes that preferentially bind to the nucleobases of RNA and DNA, thereby disrupting protein synthesis and cell proliferation, has been developed by Dunbar and co-workers [22-24]. Their research showed that the exchange of photo-labile acetonitrile ligands coordinated to the oxypyridine-bridged dirhodium core by aqua ligands could be significantly accelerated upon light irradiation and was also accompanied by a 16-fold increase in cytotoxicity. The oxygen-independent activation of those complexes is a clear advantage over established sensitizers commonly used in photodynamic therapy [24]. Soldevila-Barreda *et al.* developed a compound class based on organorhodium  $\text{Rh}(\eta^5\text{-pentamethylcyclopentadienyl})$  ( $\text{RhCp}^*$ ) complexes and their  $\text{Ru}(\eta^6\text{-}p\text{-cymene})$  analogues equipped with redox active sulfonamido ethylenediamine ligands. Those complexes showed significant catalytic activity in the conversion of  $\text{NAD}^+$  to  $\text{NADH}$  in cancer cells [25,26], indicating that the redox modulation of living cells could be an innovative concept among the new cancer treatment strategies.

Numerous studies on organometallic half-sandwich complexes have demonstrated that the type of the mono- or bidentate co-ligand(s) has a pronounced effect on physico-chemical and biological properties, such as their stability in aqueous solution and lipophilicity, which can influence cellular uptake, pharmacokinetics, and ultimately the biological activity. Therefore our research has focused on detailed analyses to illuminate correlations between complex architectures and their most important characteristics. Recently, we have reported on our investigations with  $\text{RhCp}^*$  complexes of interesting ( $\text{O}^-, \text{O}$ ) donating 3-hydroxy-4-pyrones (maltol, allomaltol) [27] and 1,2-dimethyl-3-hydroxy-pyridin-4(1*H*)-one (deferiprone, dhp) [28]. These metal complexes have shown moderate cytotoxicity with  $\text{IC}_{50}$  values in the

range of 50–165  $\mu\text{M}$  in human cancer cell lines (CH1/PA-1, SW480 and A549). A different test series wherein  $\text{RhCp}^*$  complexes formed with 2-picolinic acid (pic) [28] and the simple bidentate alkylamino and aromatic N-donor ligands, namely ethylenediamine and 2,2'-bipyridine (bpy), were examined and revealed negligible cytotoxicity [21].

Detailed solution equilibrium studies of  $\text{RhCp}^*$  complex formation with various ligands are fairly rare in the literature [29-31], especially such that provide stability constants. Our previous studies indicated that mono complexes formed with maltol and allomaltol predominate at physiological pH and decompose partially at micromolar concentrations [27]. While complexes of deferiprone, picolinic acid, ethylenediamine, bpy and 8-hydroxyquinoline are sufficiently to outstandingly stable, no direct relationship can be established between their activity and their stability in aqueous solution [28,32,33]. It is a reasonable hypothesis that the increased chloride ion affinity of  $\text{RhCp}^*$  complexes, just like in case of analogous  $\text{Ir(III)-Cp}^*$  and some  $\text{Ru(II)-arene}$  compounds [34-36], may correlate with the poor *in vitro* anticancer activity. On the other hand several other physicochemical factors such as lipophilicity, redox and kinetic properties *etc.* may influence the pharmacokinetic and pharmacodynamic behavior of a metallodrug.

Herein we investigate the effect of 6-methylation or benzene conjugation of the ( $\text{O}^-$ ,N) donor picolinic acid on the stability, lipophilicity and the biological activity of the respective  $\text{RhCp}^*$  complexes. For these studies 6-methylpicolinic acid (6-Mepic), quinoline-2-carboxylic acid (quinaldic acid, 2-QA) and 3-isoquinolinecarboxylic acid (3-iQA) (see **Chart 1**) were chosen as bidentate ligands. According to a recent study, 2-QA itself possesses antiproliferative activity [37]. The  $\text{Ru(II)}(\eta^6\text{-}p\text{-cymene})$  complex of 3-iQA has also been reported to show considerable antiproliferative potential, whereas the complex formed with 6-methylpicolinic acid (6-Mepic) exerted only low efficacy [38]. Herein, we report data on solution equilibria including complexation and chlorido/aqua co-ligand exchange processes of  $\text{RhCp}^*$  complexes of 6-Mepic (**1**), 2-QA (**2**) and 3-iQA (**3**) acquired by the combined use of pH-potentiometry,  $^1\text{H}$  NMR spectroscopy, and UV-visible (UV-Vis) spectrophotometry. The *n*-octanol/water distribution coefficients at physiological pH ( $D_{7.4}$ ) were determined for the complexes at various chloride ion concentrations. Complexes **1–3** were characterized by standard analytical methods, their biological activity was evaluated in three different human cancer cell lines and two of the complexes ( $\mathbf{1}\cdot\text{CH}_2\text{Cl}_2$  and **2**) were suitable for X-ray diffraction analysis.

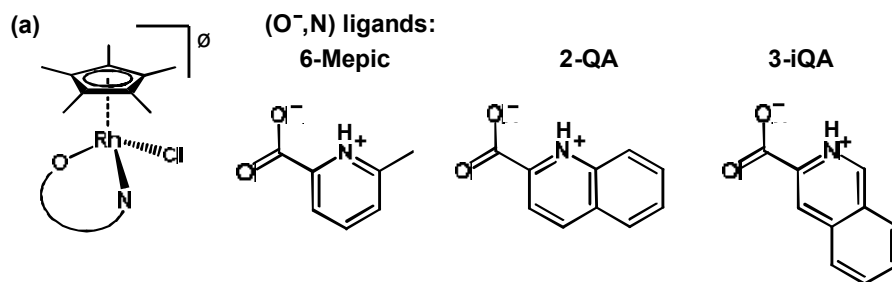


**Chart 1.** General chemical structures of the  $[\text{RhCp}^*(\text{L})\text{Cl}]$  complexes formed with 6-Mepic (**1**), 2-QA (**2**) and 3-iQA (**3**) and the chemical formulae of ligands in their neutral forms.

## Results and Discussion

### Synthesis and characterization of organometallic Rh(III) complexes

The Rh(III) precursor  $[\text{RhCp}^*(\mu\text{-Cl})\text{Cl}]_2$  was synthesized according to literature [39]. The  $\text{RhCp}^*$  complexes of 6-Mepic, 2-QA, and 3-iQA (**Chart 1**) were obtained following the established procedure described by Abbott *et al.* [40] using sodium methoxide for the deprotonation of the ligands followed by reaction with the dimeric Rh(III) precursor at room temperature. Pure compounds were isolated after extraction with  $\text{CH}_2\text{Cl}_2$ , yielding 64% (**1**), 61% (**2**) and 53% (**3**), respectively.

The organometallic Rh(III) complexes were characterized by means of standard analytical methods and their purity was verified by elemental analysis. The  $^1\text{H}$  NMR spectra of **1–3** confirm the coordination of the anionic ligand scaffolds to the organorhodium fragment, manifesting itself in a slight downfield shift of the  $\text{Cp}^*$  methyl groups and H5 of 6-Mepic. Similar observations were made for the analogous  $\text{Ru}(\text{II})(\eta^6\text{-}p\text{-cymene})$  complex of 6-Mepic [38]. In the case of the 3-iQA-based complex **3**, all ligand protons showed a more or less pronounced upfield shift upon coordination to the metal center compared to the free ligand. In general, signals representing protons next to the carboxylic group were shifted distinctly upon coordination (**Figures S1–S3**).

Single crystals of complexes  $\mathbf{1}\cdot\text{CH}_2\text{Cl}_2$  and **2** were obtained by the slow diffusion method from  $\text{CH}_2\text{Cl}_2/n\text{-hexane}$  and the results of the X-ray diffraction studies are shown in **Figures 1** and **2**, respectively. Crystallographic data are presented in **Table S1**, and selected bond lengths and angles are listed in the legends of **Figures 1** and **2** and in **Table S2**. In these complexes, Rh(III) exhibits a pseudo-octahedral geometry, where the  $\text{Cp}^*$  moiety occupies three coordination sites, the (O<sup>-</sup>,N)-donor compound binds in a bidentate manner, and the coordination sphere is completed by a chlorido ligand. Complex  $\mathbf{1}\cdot\text{CH}_2\text{Cl}_2$  crystallizes in the

monoclinic space group  $P2_1/c$ , with three molecules per asymmetric unit (**Figure 1** shows only the molecule A in the asymmetric unit for clarity; for the structures of molecules B and C see **Figure S4**), while complex **2** is a representative of the space group  $P2_12_12_1$ . The Rh to ring centroid distance of **2** (1.7655(1) Å) as well as the Rh–Cl distance (2.3991(5) Å) are similar to those calculated on average for complex **1**·CH<sub>2</sub>Cl<sub>2</sub> (1.767(1) Å and 2.405(8) Å, respectively). The measured bond lengths and angles between the metal center and the donor atoms were found in the same range as reported for the analogous picolinato complex [40]. The metal ion to ring centroid distances (**1**·CH<sub>2</sub>Cl<sub>2</sub>: 1.767(1) Å; **2**: 1.7655(1) Å) are somewhat shorter than the reported values of the picolinato complex (1.775 Å) while the Rh–N (2.1278(17) Å) and Rh–O (2.1314(15) Å) bond lengths are comparatively longer in complex **1**·CH<sub>2</sub>Cl<sub>2</sub>. In the picolinato complex, distances of 2.117(3) and 2.108(2) Å were obtained for the Rh–N and Rh–O bonds, respectively and are in the same range as bond lengths found in complex **2** (Rh–N: 2.1343(16) Å, Rh–O: 2.0991(13) Å) [40]. In complex **1**·CH<sub>2</sub>Cl<sub>2</sub> the ligand 6-Mepic forms a five-membered chelate ring (N1/C1/C6/O1/Rh1) which adopts a Rh1-endo envelope conformation with an average deflection angle of  $\varphi = 20.9(7)^\circ$  measured between the planes defined by N1–C1–C6–O1 and N1–Rh1–O1 atoms (see **Figure S5**). This phenomenon can be explained by the increased steric demand of the methyl group which forces a turn out-of-plane of the chelate ring. For complex **2** a significantly smaller angle was found ( $\varphi = 9.77^\circ$ ). Compared to those values, the torsion out-of-plane found for the comparable chelate ring in the picolinato complex is rather small ( $\varphi = 3.37^\circ$ ) [40].

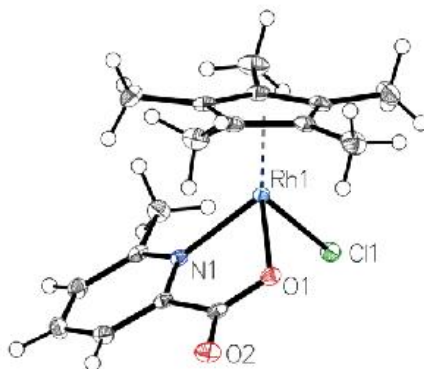


**Figure 1.** ORTEP view of complex **1**·CH<sub>2</sub>Cl<sub>2</sub> with 50% displacement ellipsoids. Solvent molecules and two further independent molecules in the asymmetric unit are omitted for clarity. Selected bond distances (Å) and angles (deg): Rh1–N1: 2.1278(17); Rh1–O1: 2.1314(15); Rh1–Cl1: 2.3960(5); Rh1–ring centroid: 1.7664(1); N1–Rh1–O1: 76.98(6)°; N1–Rh1–Cl1: 90.39(5)°; O1–Rh1–Cl1: 90.97(4)°; structures and data for the two other molecules are listed in **Figure S4** and **Table S2**.

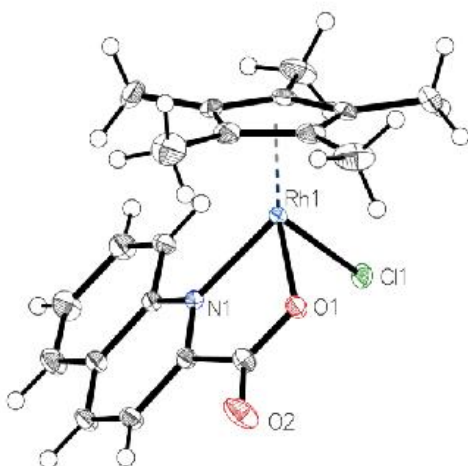


**Figure 2.** ORTEP view of complex **2** with 50% displacement ellipsoids. Selected bond distances (Å) and angles (deg): Rh1–N1: 2.1343(16); Rh1–O1: 2.0991(13); Rh1–Cl1: 2.3991(5); Rh1–ring centroid: 1.7655(1); N1–Rh1–O1: 77.29(6)°; N1–Rh1–Cl1: 85.33(4)°; O1–Rh1–Cl1: 91.55(4)°.

## Proton dissociation processes of the studied ligands and hydrolysis of the $[\text{RhCp}^*(\text{H}_2\text{O})_3]^{2+}$ organometallic cation

Proton dissociation constants of the ligands 6-Mepic, 2-QA and 3-iQA were determined by pH-potentiometry and  $^1\text{H}$  NMR spectroscopy (**Table 1**), and are in reasonably good agreement with data acquired under similar conditions reported in literature [41,42]. The proton dissociation constant can be attributed to the deprotonation of the quinolinium ( $\text{NH}^+$ ) group. The carboxylate remains completely deprotonated in the studied pH range (pH = 0.7–11.5). 2-QA has a lower  $\text{p}K_a$  than 3-iQA, a finding that follows the well-known trend for the  $\text{p}K_a$  values of the reference compounds: quinoline and isoquinoline [43,44].

Hydrolytic behavior of the aquated organometallic cation  $[\text{RhCp}^*(\text{H}_2\text{O})_3]^{2+}$  has been studied previously [27,29], and the structure of the major hydrolysis product,  $[(\text{RhCp}^*)_2(\mu\text{-OH})_3]^+$ , was characterized by single-crystal X-ray analysis [45]. Overall stability constants for the  $\mu$ -hydroxido-bridged dinuclear species ( $[(\text{RhCp}^*)_2(\mu\text{-OH})_3]^+$  and  $[(\text{RhCp}^*)_2(\mu\text{-OH})_2]^{2+}$ ) measured at various ionic strengths were reported in our previous work [27].

## Complex formation equilibria of $[\text{RhCp}^*(\text{H}_2\text{O})_3]^{2+}$ with 6-Mepic, 2-QA and 3-iQA

Complex formation with the three different ligands was investigated by the combined use of pH-potentiometry,  $^1\text{H}$  NMR and UV-Vis spectroscopy. The stoichiometry of the formed complexes and the equilibrium constants furnishing the best fits to the experimental data are listed in **Table 1**. Stability data for the formerly studied analogous complex with picolinic acid are shown here as well for comparison [28]. Notably, the complex formation under these conditions was found to be fast and took place within 5-10 minutes for the studied complexes.

Representative pH-potentiometric titration curves of the  $[\text{RhCp}^*(\text{H}_2\text{O})_3]^{2+}$  – 3-iQA system are shown in **Figure 3**. The titration data revealed almost complete displacement of the quinolinium proton by the metal ion due to complex formation already at pH 2; accordingly the titration curve containing 1:1 ligand-to-metal ion has the shape of a strong acid–strong base titration curvature up to pH ~7. Titration points at pH > 7 initiate various processes parallel to the deprotonation of the coordinated water in  $[\text{RhCp}^*(\text{L})(\text{H}_2\text{O})]^+$  (L= deprotonated form of the ligand) resulting in the formation of species of the form  $[\text{RhCp}^*(\text{L})(\text{OH})]$  (see **Chart S1**). Based on the obtained data decomposition of the complex might take place as well, giving rise to the hydroxido-bridged compound  $[(\text{RhCp}^*)_2(\mu\text{-OH})_3]^+$ , a process that is accompanied by ligand release [27].



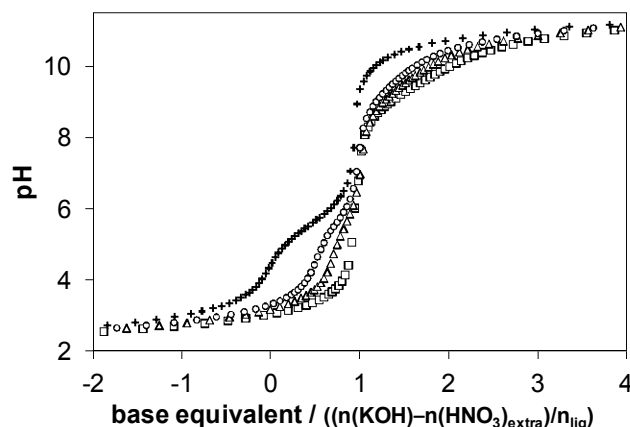


**Figure 3.** Representative pH-potentiometric titration curves of the  $[\text{RhCp}^*(\text{H}_2\text{O})_3]^{2+}$  – 3-iQA system in aqueous solution at various metal-to-ligand ratios. Symbols: free ligand (+); 1:2 (o); 1:1.5 ( $\Delta$ ) and 1:1 ( $\square$ ).  $\{C_{\text{ligand}} = 1.0 \text{ mM}; T = 25 \text{ }^\circ\text{C}; I = 0.20 \text{ M (KNO}_3)\}$ .

UV-Vis spectra recorded at highly acidic conditions (pH  $\sim$  0.7) showed no decomposition of the complex **3** (0.1 mM) due to its high stability. Thus, the stability constant for this species was determined by ligand competition measurements using spectrophotometry at pH 7.4. Ethylenediamine was chosen as competitor since the stability constants for the  $\text{RhCp}^*$  – ethylenediamine complex were acquired under the same conditions as applied in this study [32]. Upon addition of ethylenediamine to a sample containing  $[\text{RhCp}^*(\text{H}_2\text{O})_3]^{2+}$  and 3-iQA at 1:1 metal-to-ligand ratio, clear UV-Vis spectral changes were observed (**Figure 4**).

The stepwise displacement of the originally metal-bound 3-iQA by ethylenediamine results in the formation of complex  $[\text{RhCp}^*(\text{en})(\text{H}_2\text{O})]^+$ , thus unbound 3-iQA and excess amounts of ethylenediamine (making no contribution to the measured absorbance) are present in the sample. The stability constant of **3** could be calculated by deconvolution of the recorded spectra using the computer program PSEQUAD [46]. Including this value as a fixed constant, the  $\text{pK}_a$  of the mono complex could be calculated from the pH-potentiometric titration data (**Table 1**).

**Table 1.** Proton dissociation constants ( $pK_a$ ) of the studied ligands and overall stability constants ( $\log\beta$ ),  $pK_a$ , and  $pM_{7.4}$  values of their  $[RhCp^*(L)(H_2O)]^+$  complexes in chloride-free aqueous solutions determined by various methods,  $H_2O/Cl^-$  exchange constants ( $\log K'$ ) for the same complexes, and the  $^1H$  NMR chemical shifts of  $CH_3(Cp^*)$  protons of the indicated complexes  $\{T = 25\text{ }^\circ C; I = 0.2\text{ M (KNO}_3)\}$ .<sup>[a]</sup>

	method	L: pic <sup>[b]</sup>	6-Mepic 1	2-QA 2	3-iQA 3
$pK_a$ (HL)	<i>pH-metry</i>	5.21	5.89(1)	4.83(1)	5.62(2)
	$^1H$ NMR	–	5.91(1)	4.79(1)	5.57(2)
$\log\beta$ $[RhCp^*(L)(H_2O)]^+$	<i>pH-metry</i>	9.18	9.79(7)	9.49(4)	10.60(3) <sup>[c]</sup>
$pK_a$ $[RhCp^*(L)(H_2O)]^+$	<i>pH-metry</i>	9.32	9.49(10)	9.31(5)	9.26(1)
	$^1H$ NMR	9.38	9.54(1)	9.42(1)	9.49(1)
$pM_{7.4}$ <sup>[d]</sup>		5.35	5.76	5.57	6.29
$\log K'$ $(H_2O/Cl^-)$ <sup>[e]</sup>	<i>UV-Vis</i>	2.20	2.10(1)	2.33(1)	2.05(1)
$\delta CH_3(Cp^*)$ (ppm)	$[RhCp^*(L)(H_2O)]^+$	1.70	1.63	1.62	1.74
	$[RhCp^*(L)(OH)]$	1.65	1.57	1.56	1.68

[a] Standard deviations (SD) are in parenthesis. Hydrolysis products of the organometallic cation:  $\log\beta [(RhCp^*)_2(\mu-OH)_2]^{2+} = -8.53$ ,  $\log\beta [(RhCp^*)_2(\mu-OH)_3]^+ = -14.26$  at  $I = 0.20\text{ M (KNO}_3)$  taken from Ref. [27]. [b] Taken from Ref. [28]. [c] Determined by UV-Vis spectrophotometry via competition studies measured at pH 7.40, the competitor ligand was ethylenediamine see details in experimental section. [d]  $pM_{7.4} = -\log[M]$ , where  $[M]$  is the equilibrium concentration of the ligand-free, unbound metal ion in its different forms:  $[RhCp^*(H_2O)_3]^{2+}$ ,  $[(RhCp^*)_2(\mu-OH)_i]^{(4-i)+}$  ( $i = 2$  or  $3$ )  $\{C_M = 1\text{ mM; M:L} = 1:1, \text{pH} = 7.4\}$ . [e] For the  $[RhCp^*(L)(H_2O)]^+ + Cl^- \rightleftharpoons [RhCp^*(L)Cl] + H_2O$  equilibrium determined at various total chloride ion concentrations by UV-Vis.

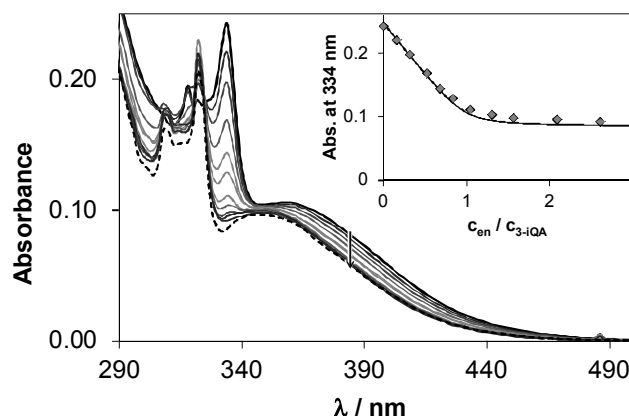


**Figure 4.** UV-Vis spectra of the  $[\text{RhCp}^*(\text{H}_2\text{O})_3]^{2+}$  – 3-iQA – ethylenediamine system recorded at pH 7.40 at various ethylenediamine-to-3-iQA ratios (dashed spectrum is calculated as the sum of the spectra of  $[\text{RhCp}^*(\text{ethylenediamine})(\text{H}_2\text{O})]^{2+}$  and 3-iQA). Inset shows the measured ( $\blacklozenge$ ) and fitted (solid line) absorbance values at 334 nm plotted against the ethylenediamine (en)-to-3-iQA ratios. Spectra are background subtracted spectra.  $\{C_{\text{RhCp}^*} = C_{3\text{-iQA}} = 99 \mu\text{M}; C_{\text{ethylenediamine}} = 0\text{--}148 \mu\text{M}; \text{pH} = 7.40$  (20 mM phosphate buffer);  $T = 25 \text{ }^\circ\text{C}$ ; incubation time = 24 h;  $I = 0.20 \text{ M (KNO}_3)$   $l = 0.5 \text{ cm}$ )

In order to investigate equilibrium processes,  $^1\text{H}$  NMR titrations were carried out. The NMR spectra in **Figure 5** show one set of peaks at pH values varying between 1.97 and 8.13 which confirm the predominant formation of complex **3** as neither unbound 3-iQA nor Rh(III)-Cp\* fragment can be detected in this pH range. At  $\text{pH} > 7.75$ , an equilibrium between the aquated complex and the mixed hydroxido species  $[\text{RhCp}^*(\text{L})(\text{OH})]$  is reached, with very high exchange rates that cannot be resolved in the NMR time scale. These exchange processes cause a high field shift of proton resonances, thereby providing a means of calculation of the  $\text{pK}_a$  value of the complex (**Table 1**).

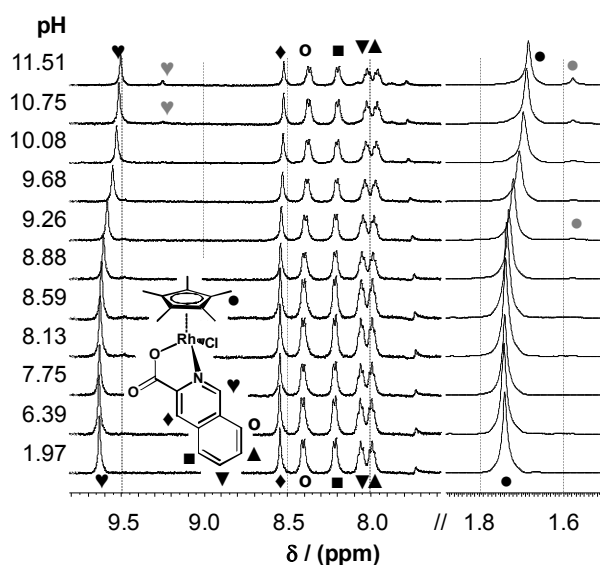


**Figure 5.**  $^1\text{H}$  NMR spectra of the  $[\text{RhCp}^*(\text{H}_2\text{O})_3]^{2+} - 3\text{-iQA}$  (1:1) system in aqueous solution recorded at the indicated pH values; peak assignment is indicated in the figure for the complex bound (black symbols) and unbound (grey symbols) species  $\{c_{\text{RhCp}^*} = c_{3\text{-iQA}} = 1 \text{ mM}; T = 25 \text{ }^\circ\text{C}; I = 0.20 \text{ M (KNO}_3\text{); } 10\% \text{ D}_2\text{O}\}$ .

Furthermore, peaks of the hydroxido-bridged dimer  $[(\text{RhCp}^*)_2(\mu\text{-OH})_3]^+$  as well as peaks representing the deprotonated free ligand 3-iQA appear at  $\text{pH} > 9.26$  (**Figure 5**). However, fairly low peak integrals indicate the rather small extent to which the complexes decompose.

Concentration distribution curves were computed including the stability constants determined by competition measurements and pH-potentiometric titrations. Acquired data are in good agreement with the molar fractions calculated on the basis of NMR peak integrals along with the chemical shift values of the  $\text{Cp}^*$  methyl protons (**Figure 6**).

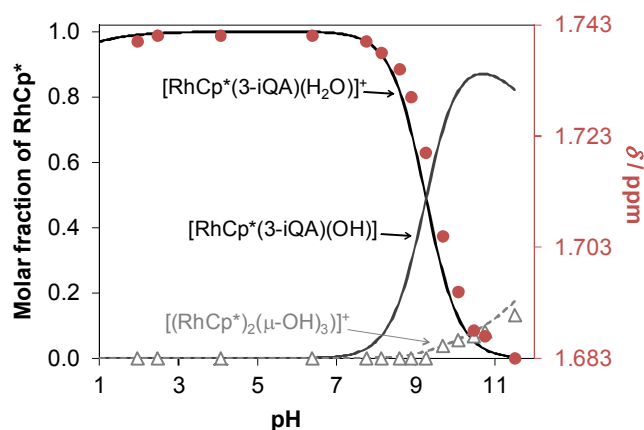


**Figure 6.** Concentration distribution curves (solid lines) for the  $[\text{RhCp}^*(\text{H}_2\text{O})_3]^{2+} - 3\text{-iQA}$  (1:1) system in aqueous solution calculated on the basis of the stability constants determined and the  $^1\text{H}$  NMR peak integrals for the  $\text{Cp}^*$  methyl protons of  $[(\text{RhCp}^*)_2(\mu\text{-OH})_3]^+$  ( $\Delta$ ), and pH-dependent chemical shift values ( $\bullet$ ) of the  $\text{Cp}^*$  methyl protons.  $\{c_{\text{RhCp}^*} = c_{3\text{-iQA}} = 1 \text{ mM}; T = 25 \text{ }^\circ\text{C}; I = 0.20 \text{ M (KNO}_3\text{); } 10\% \text{ D}_2\text{O}\}$ .

A similar solution speciation model was applied in the case of complexes **1** and **2**. Stability constants could be computed from the pH-potentiometric data directly and were found to be somewhat lower than those obtained for **3** (**Table 1**). It can be concluded that the deprotonation constants ( $\text{p}K_a$ ) of **1–3** are fairly high in all cases, and the aqua complex is the predominant form ( $\sim 99\%$ ) at physiological pH. Instead of the direct comparison of stability constants,  $\text{pM}$  values were calculated at various pH values (see **Table 1** and **Figure S6**). The  $\text{pM}$  value, which is defined as the negative logarithm of the equilibrium concentrations of the unbound metal ion under the given conditions (pH, analytical concentrations of the ligand and metal ion), was introduced by Raymond *et al.* [47] to gauge the relative affinities of

ligands towards a metal ion. A higher pM value indicates a stronger metal ion binding ability. In our case both the organometallic cation  $[\text{RhCp}^*(\text{H}_2\text{O})_3]^{2+}$  as well as the  $\mu$ -hydroxido dinuclear complexes  $[(\text{RhCp}^*)(\mu\text{-OH})_i]^{(4-i)+}$  ( $i = 2$  or  $3$ ) have to be considered as unbound species. In this way we take into account equilibria occurring simultaneously with the metal-ligand complex formation such as (de)protonation processes of the ligand, and hydrolysis of the organometallic fragment. The calculations reveal the following stability trend at physiological pH: pic < 2-QA < 6-Mepic  $\ll$  3-iQA (**Table 1**). Thus, the extension of the picolinic acid structure by 6-methylation or benzene conjugation increases the complex stability of the respective  $\text{RhCp}^*$  derivatives. The three investigated ligands form  $\text{RhCp}^*$  complexes of pronounced stability. Based on their stability constants, decomposition does not occur even at low micromolar concentrations to a measurable extent. This assumption was confirmed both in chloride free and 0.2 M KCl containing aqueous solution, using the  $\text{RhCp}^* - 3\text{-iQA}$  system in a 1:1 ratio: a dilution series (from 2 mM down to 4  $\mu\text{M}$ ) was prepared at pH 7.40 and the recorded UV-Vis spectra, after normalization, were identical under the applied conditions, which indicates that there is no complex decomposition in the studied concentration range (see **Figure S7**).

With the help of pM values, we can directly compare the  $\text{RhCp}^*$  binding abilities of the studied ligands and previously studied ( $\text{O}^-,\text{O}$ ) donating ligand deferiprone and the (N,N) donating 2,2'-bipyridine (**Figure S6**), thus the solution stabilities of the complexes become comparable under the given conditions. The  $\text{pM}_{7.4}$  value of **2** is more than half an order of magnitude higher compared to that of the  $\text{RhCp}^*$  deferiprone complex with an ( $\text{O}^-,\text{O}$ ) coordination mode (4.99 [28]), but more than two orders of magnitude lower than the  $\text{pM}_{7.4}$  value of the 2,2'-bipyridine complex (7.82 [32]).

### Chloride ion affinity and lipophilicity of the $[\text{RhCp}^*(\text{L})(\text{H}_2\text{O})]^+$ complexes

Beside metal complex stability, many other factors impact the pharmacological behavior. Complete or partial displacement of the chloride ion by an aqua ligand (**Chart S1**) is considered a crucial step in the activation process of half-sandwich complexes. The aquation of the well-known anticancer drug cisplatin has been thoroughly studied and the aquated form of the complex was identified as the active species. This hydrolysis is controlled both kinetically and thermodynamically; the thermodynamic driving force is thought to be the gradient in chloride ion concentration (chloride ion content in blood serum: 100 mM > cell plasma: ~24 mM > cell nucleus: ~4 mM) [48]. A dependence of cytotoxic efficacy on chloride ion affinity has been observed for several  $[\text{Ru}(\text{II})(\eta^6\text{-arene})]$  complexes [49-51]. In the case

of the studied RhCp\* complexes of the form  $[\text{Rh}(\text{Cp}^*)(\text{L})(\text{H}_2\text{O})]^+$  (similarly to previously characterized complexes [27,28,32]) the chloride-water exchange process was found to be fast and takes place within a few minutes. **Figure S8** shows the spectral changes of **1** upon the increase in chloride ion concentration. The  $\log K' (\text{H}_2\text{O}/\text{Cl}^-)$  constants (**Table 1**) were calculated by the deconvolution of UV-Vis spectra and were found to be significantly high ( $>2$ ), thus they represent a strong affinity of these complexes towards the chloride ions. With the aid of aqua/chlorido exchange constants, we can estimate the ratio of the aqua and the chlorido complexes at chosen chloride ion concentrations. At a chloride concentration of 100 mM, 92% of **3** and 96% of **2** appear in the neutral chlorido form, while at chloride ion concentrations comparable to those of the cell nucleus (4 mM), 69% and 54% of these complexes are present as the more reactive aqua species.

One other notable consequence of the aqua/chlorido exchange equilibrium is the altered net charge of the complexes (see **Chart S1**). Since the lipo/hydrophilic character of a compound is strongly influenced by its charge, distribution coefficients at pH 7.4 ( $D_{7.4}$ ) were determined for **1–3** (and additionally for the picolinate complex for comparison) at various chloride ion concentrations.

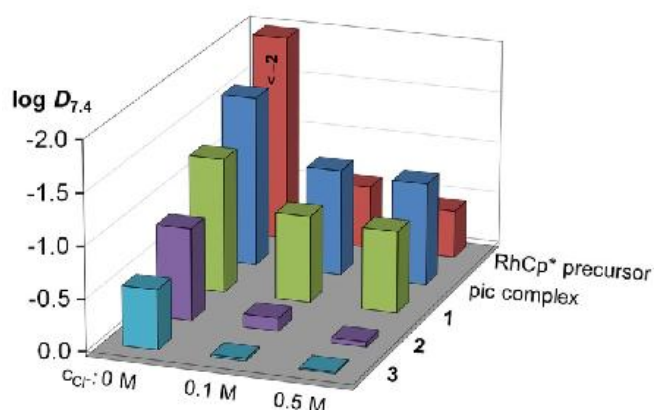


**Figure 7.** Logarithm of distribution coefficients ( $\log D_{7.4}$ ) of the RhCp\* precursor,  $[\text{RhCp}^*(\text{pic})(\text{H}_2\text{O})]^+$  and complexes **1–3** at pH 7.40 measured at various KCl concentrations (as indicated in the figure)  $\{C_{\text{compound}} = 200 \mu\text{M}; T = 25 \text{ }^\circ\text{C}, \text{ in } 20 \text{ mM phosphate buffer}\}$ . Log  $D_{7.4}$  values of the ligands measured at 0.1 M KCl content for comparison: 2-QA:  $-1.3(1)$ , 3-iQA:  $-1.41(4)$  and pic:  $<-2.0$  [52], 6-Mepic:  $<-2.0$  [52].

**Figure 7** (and **Table S3**) illustrates the  $\log D_{7.4}$  values of the complexes and the RhCp\* precursor at varying KCl concentrations and those of the respective ligands. The ligands pic and 6-Mepic definitely possess hydrophilic character owing to the deprotonated carboxylate group, while 2-QA and 3-iQA are somewhat less hydrophilic due to the more extended

aromatic structure. The organorhodium fragment RhCp\* itself displays a chloride ion dependent lipo/hydrophilic character: less than 1% of RhCp\* is detected in the *n*-octanol phase in chloride ion free solution ( $\log D_{7.4} < -2$ ), while in the presence of 0.1 M KCl already a significant amount (20%) is found in the organic phase ( $\log D_{7.4} = -0.61(6)$ ). The ratio slightly increases at a concentration of 0.50 M KCl (26%,  $\log D_{7.4} = -0.46(3)$ ). Considering the hydrolysis tendency of the organometallic cation  $[\text{RhCp}^*(\text{H}_2\text{O})_3]^{2+}$  at pH 7.4 not primarily the water-chlorido but the hydroxido-chlorido exchange and consequently a dimer-monomer redistribution is the predominant process. In our studies the lipophilic character of **1–3** was found to increase in the following order (independent of absence or presence of chloride ions): pic complex < **1** << **2** < **3**, analogous to the lipophilicity of the free ligands. Moreover,  $\log D_{7.4}$  values obtained for the complexes in the presence of 0.10 M KCl, are distinctly higher (0.6–0.7 orders of magnitude) than values acquired in samples without chloride ions.

It is noteworthy that the lipo/hydrophilic character of the complexes is not only affected by the type of the ligands but also by their affinity for chloride ions and the chloride ion concentration in solution. This feature may facilitate cell accumulation of the complexes via passive transport since the chlorinated complex can pass easier across the cell membrane compared to its charged, aquated form.

### **Cytotoxic activity in cancer cell lines**

In our previous work, RhCp\* complexes bearing the hydroxypyron ligands maltol and allomaltol, the hydroxypyridinone derivative deferiprone, picolinic acid and 8-hydroxyquinoline, were investigated with regard to their anticancer potential in various human cancer cell lines [27,28,33]. These complexes were found to exhibit minor cytotoxicity with the exception of the deferiprone and 8-hydroxyquinoline-based complexes. In general, no correlation was observed between the IC<sub>50</sub> values and the calculated pM values, implying an independence of cytotoxicity from solution stability. The pK<sub>a</sub> values of the complexes are rather high, hence the lack of cytotoxicity cannot be associated with the formation of the less active mixed hydroxido species at pH 7.4 [50]. At the same time the analogous Ru(II)( $\eta^6$ -*p*-cymene) picolinato complex resulted in IC<sub>50</sub> values of 36–82  $\mu\text{M}$  measured in human cancer cell lines, such as cervix carcinoma (HeLa) and melanoma cells (FemX) [53]. Cytotoxicity data for the related Ru(II)( $\eta^6$ -*p*-cymene) complexes of 6-Mepic and 3-iQA have been acquired and published previously. The 3-iQA-based Ru(II) complex shows moderate activity in HeLa (45.35  $\mu\text{M}$ ), FemX (18.48  $\mu\text{M}$ ) and A549 (25.76  $\mu\text{M}$ ) cells. Furthermore, a high IC<sub>50</sub> value in normal cells (MRC-5, 84.18  $\mu\text{M}$ ) supports its tumor selective cytotoxic activity [38]. On the other hand the Ru(II)( $\eta^6$ -*p*-cymene) complex of 6-Mepic showed low activity in the same cell lines (HeLa: 278  $\mu\text{M}$ , FemX: 169  $\mu\text{M}$ , A549: > 300  $\mu\text{M}$ ) [38]. The cytotoxic activity of

RhCp\* complexes **1–3** and the corresponding free ligands have been evaluated by means of the colorimetric MTT assay (MTT = 3-(4,5-dimethyl-2-thiazolyl)-2,5-diphenyl-2*H*-tetrazolium bromide) in the human cancer cell lines A549 (non-small cell lung cancer), SW480 (colon carcinoma) and CH1/PA-1 (ovarian teratocarcinoma). In general no considerable activity of the complexes was found with the exception of complex **3** in CH1/PA-1 cells (**Table 2**). Cytotoxic potency of the free ligands is poor to virtually non-existent, with only 3-iQA yielding IC<sub>50</sub> values in the tested range of up to 400 μM. One possible reason for poor anticancer activities of compounds **1–3** could be an impeded aquation due to the exceptionally high affinity of the complexes for chloride ions. This correlation has already been pointed out for related Ru(II), Os(II) and Ir(III) complexes [34-36]. However, high chloride ion affinity may hinder not only the aquation of the complexes but also possible monodentate coordination of bio-ligands (such as proteins or DNA nucleobases). Additionally, other physico-chemical properties such as lipophilicity or redox activity *etc.* can influence the cytotoxic activity. Consequently, the increased lipophilicity and higher stability in solution found for complex **3** (*vide supra*) as well as a certain cytotoxic potency inherent in the 3-iQA ligand *per se* might contribute to its higher cytotoxicity in CH1/PA-1 cells.

**Table 2.** *In vitro* cytotoxicity (IC<sub>50</sub> values in μM in three human cancer cell lines) of the RhCp\* complexes of 6-Mepic (**1**), 2-QA (**2**) and 3-iQA (**3**) and pic as well as the corresponding free ligands for comparison.<sup>[a]</sup>

IC <sub>50</sub> [μM]	A549	SW480	CH1/PA-1
RhCp* Complexes			
<b>1</b> (6-Mepic)	356 ± 36	319 ± 38	221 ± 19
<b>2</b> (2-QA)	>200	>100	115 ± 36
<b>3</b> (3-iQA)	174 ± 5	161 ± 7	10.2 ± 0.4
pic <sup>[b]</sup>	343 ± 24	283 ± 65	258 ± 6
Ligands			
<b>6-Mepic</b>	>400	>400	>400
<b>2-QA</b>	>400	>400	>400
<b>3-iQA</b>	288 ± 14	360 ± 35	85 ± 11

[a] 96 h exposure. [b] Data taken from Ref. [28].

## Conclusions

The evaluation of stability and speciation of organometallic compounds is of high value for the assessment of their behavior under physiological conditions. Data presented within this work were acquired by the application of a variety of methods, comprising <sup>1</sup>H NMR and UV-Vis spectroscopy, pH potentiometry, X-ray diffraction analysis and cytotoxicity tests. By



means of these methods we could demonstrate exclusive formation of the mono-ligand complexes, such as  $[\text{RhCp}^*(\text{L})(\text{H}_2\text{O})]^+$  (L = deprotonated 6-Mepic, 2-QA or 3-iQA) and  $[\text{RhCp}^*(\text{L})(\text{OH})]$ , depending on the pH. Formation of the hydroxido complexes could be characterized by determination of relatively high  $pK_a$  values ( $> 9.25$ ), while complexes of the form  $[\text{RhCp}^*(\text{L})(\text{H}_2\text{O})]^+$  predominate at physiological pH even in the micromolar concentration range. The ligand 3-iQA forms complexes of the highest stability with  $\text{RhCp}^*$  in this series. In general, the stability of the complexes formed with all three ligands significantly exceeds that of hydroxypyridinones, such as maltol or deferiprone, although it stays below the stability of complexes with (N,N) donor ligands such as ethylenediamine or 2,2'-bipyridine.

Chloride ions acting as competitive ligands are able to suppress the aquation to some extent. This process may play an important role in the mechanism of action of this type of organometallic complexes. The extent of the chloride/water exchange was shown to depend on the chloride concentrations in the medium as well as on the thermodynamic exchange constant.  $\text{H}_2\text{O}/\text{Cl}^-$  co-ligand exchange constants for the complexes **1–3** were determined, and all compounds are able to retain the chlorido ligand at the third coordination site to an extent comparable to that of  $\text{RhCp}^*$  complexes with picolinic acid, ethylenediamine or 2,2'-bipyridine. Based on these constants it can be predicted that more than 90% of the respective complexes exist as the chlorido complex at the chloride concentration corresponding to those in human blood serum. As a consequence of the replacement of the aqua ligand by a chlorido ligand, the net charge of the complexes changes from +1 to neutral, thus the co-ligand exchange strongly influences their lipophilicity. It can therefore be assumed that the higher chloride ion content results in a more lipophilic character. The fact that minor cytotoxic effects were observed in *in vitro* tests performed with complexes **1–3** could be explained by the high affinity of complexes for chloride ions which might suppress the activation of the investigated compounds.

Overall, the extension of the picolinic acid structure by 6-methylation or annellation of a benzene ring results in increased stability and lipophilicity of the synthesized  $\text{RhCp}^*$  complexes, but the influence on the anticancer properties is only minor.

## Experimental Section

### Materials

All solvents were of analytical grade and used without further purification. 6-Mepic, 2-QA, 3-iQA, KCl,  $\text{KNO}_3$ ,  $\text{AgNO}_3$ , HCl,  $\text{HNO}_3$ , KOH, 4,4-dimethyl-4-silapentane-1-sulfonic acid (DSS),  $\text{NaH}_2\text{PO}_4$ ,  $\text{Na}_2\text{HPO}_4$  and ethylenediamine were purchased from Sigma-Aldrich in *puriss*

quality.  $\text{RhCl}_3$  was purchased from Johnson Matthey. Doubly distilled Milli-Q water was used for sample preparation. The dimeric rhodium precursor [rhodium(III)( $\eta^5$ -1,2,3,4,5-pentamethylcyclopentadienyl)( $\mu$ -Cl)Cl] $_2$  ( $[\text{RhCp}^*(\mu\text{-Cl})\text{Cl}]_2$ ) was prepared according to literature procedures [39]. The exact concentration of the ligand stock solutions together with the proton dissociation constants were determined by pH-potentiometric titrations with the use of the computer program HYPERQUAD [54]. The aqueous  $[\text{RhCp}^*(\text{H}_2\text{O})_3](\text{NO}_3)_2$  stock solution was obtained by dissolving an exact amount of  $[\text{RhCp}^*(\mu\text{-Cl})\text{Cl}]_2$  in water followed by the removal of chloride ions by addition of equivalent amounts of  $\text{AgNO}_3$ . The exact concentration of  $[\text{RhCp}^*(\text{H}_2\text{O})_3]^{2+}$  was determined by pH-potentiometric titrations employing stability constants for  $[(\text{RhCp}^*)_2(\mu\text{-OH})_i]^{(4-i)+}$  ( $i = 2$  or  $3$ ) complexes [27].

## Synthesis of $\text{RhCp}^*$ complexes with 6-Mepic, 2-QA and 3-iQA

### General procedure for the synthesis of complexes 1-3

The ligand (1 eq) and sodium methoxide (1.1 eq) were dissolved in dry methanol (10 mL) and after stirring at room temperature for 15 min,  $[\text{RhCp}^*(\mu\text{-Cl})\text{Cl}]_2$  (0.9 eq) was added. The mixture was stirred under argon atmosphere and at room temperature for 24 h. The solvent was subsequently removed under reduced pressure; the obtained residue was taken up in  $\text{CH}_2\text{Cl}_2$  and filtered to remove insoluble reaction by-products. The filtrate was concentrated to a volume of 2 mL under reduced pressure. Precipitation with *n*-hexane afforded the desired product in moderate to good yields (53–64%).

$^1\text{H}$  NMR spectra were recorded at 25 °C and 500.10 MHz and  $^{13}\text{C}\{\text{H}\}$  NMR spectra at 25 °C and 125.75 MHz using a Bruker FT-NMR spectrometer Avance III™ 500 MHz. For the characterization with NMR spectroscopy  $\text{CDCl}_3$  was used as solvent. Elemental analyses were carried out on a Perkin Elmer 2400 CHN Elemental Analyser at the Microanalytical Laboratory (University of Vienna). If not stated otherwise, the substances were synthesized and purified according to general procedures.

### Chlorido[(6-methylpyridine- $\kappa\text{N}$ -2-carboxylato- $\kappa\text{O}$ )( $\eta^5$ -1,2,3,4,5-

pentamethylcyclopentadienyl)rhodium(III)] (1): The reaction was performed according to the general procedure using 6-Mepic (74 mg, 0.54 mmol), sodium methoxide (32 mg, 0.594 mmol) and  $[\text{RhCp}^*(\mu\text{-Cl})\text{Cl}]_2$  (150 mg, 0.243 mmol). The product was obtained as orange crystals. Yield: 127 mg (64%);  $^1\text{H}$  NMR (500.10 MHz,  $\text{CDCl}_3$ )  $\delta$  7.98 (d,  $^3J$  (H,H) = 8 Hz, 1H, CH3); 7.80 (dd,  $^3J$  (H,H) = 8 Hz,  $^3J$  (H,H) = 8 Hz, 1H, CH4); 7.47 (d,  $^3J$  (H,H) = 8 Hz, 1H, CH5); 2.92 (s, 3H, CH<sub>3</sub>); 1.67 (s, 15H, CH<sub>3,Cp</sub><sup>\*</sup>) ppm.  $^{13}\text{C}$  NMR (125.75 MHz,  $\text{CDCl}_3$ )  $\delta$  170.6 (C7); 159.4 (C6); 153.4 (C2); 139.0 (CH4); 128.3 (CH5); 124.6 (CH3); 94.1 (d,  $^1J$ (Rh,C) =

9 Hz, C<sub>Cp\*</sub>); 26.5 (CH<sub>3,6-Mepic</sub>); 9.3 (CH<sub>3,Cp\*</sub>) ppm. Elemental analysis for C<sub>17</sub>H<sub>21</sub>ClNO<sub>2</sub>Rh·0.5 H<sub>2</sub>O calc. C 48.76, H 5.30, N 3.35; found C 48.41, H 5.31, N 3.40.

**Chlorido[(2-quinoline-κN-carboxylato-κO)(η<sup>5</sup>-1,2,3,4,5-**

**pentamethylcyclopentadienyl)rhodium(III)] (2):** The reaction was performed according to the general procedure using 2-QA (94 mg, 0.54 mmol, 1 eq), sodium methoxide (32 mg, 0.594 mmol, 1.1 eq) and [RhCp\*(μ-Cl)Cl]<sub>2</sub> (150 mg, 0.243 mmol, 0.45 eq). The product was obtained as orange crystals. Yield: 132 mg (61%); <sup>1</sup>H NMR (500.10 MHz, CDCl<sub>3</sub>) δ 8.46 (d, <sup>3</sup>J (H,H) = 9 Hz, 1H, CH8); 8.38 (d, <sup>3</sup>J (H,H) = 9 Hz, 1H, CH4); 8.22 (d, <sup>3</sup>J (H,H) = 9 Hz, 1H, CH3); 7.95 (d, <sup>3</sup>J (H,H) = 9 Hz, 1H, CH5); 7.90 – 7.86 (m, 1H, CH6); 7.74 – 7.70 (m, 1H, CH7); 1.65 (CH<sub>3,Cp\*</sub>) ppm. <sup>13</sup>C NMR (125.75 MHz, CDCl<sub>3</sub>) δ 170.5 (C9); 154.5 (C2); 145.2 (C8a); 139.9 (CH4); 131.2 (CH7); 131.1 (C4a); 129.4 (CH8); 129.1 (CH6); 128.9 (CH5); 123.3 (CH3); 94.3 (d, <sup>1</sup>J(Rh,C) = 9 Hz, C<sub>Cp\*</sub>); 9.3 (CH<sub>3,Cp\*</sub>) ppm. Elemental analysis for C<sub>20</sub>H<sub>21</sub>ClNO<sub>2</sub>Rh calc. C 53.89, H 4.75, N 3.14; found C 53.61, H 4.66, N 3.26

**Chlorido[(3-isoquinoline-κN-carboxylato-κO)(η<sup>5</sup>-1,2,3,4,5-**

**pentamethylcyclopentadienyl)rhodium(III)] (3):** The reaction was performed according to the general procedure using 3-iQA acid (94 mg, 0.54 mmol, 1 eq), sodium methoxide (32 mg, 0.594 mmol, 1.1 eq) and [RhCp\*(μ-Cl)Cl]<sub>2</sub> (150 mg, 0.243 mmol, 0.90 eq). The product was obtained as orange crystals. Yield: 115 mg (53%); <sup>1</sup>H NMR (500.10 MHz, CDCl<sub>3</sub>) δ 9.23 (s, 1H, CH1); 8.48 (s, 1H, CH4); 8.08 (d, <sup>3</sup>J (H,H) = 8 Hz, 1H, CH8); 7.96 (d, <sup>3</sup>J (H,H) = 8 Hz, 1H, CH5); 7.86 – 7.81 (m, 1H, CH6); 7.78 – 7.74 (m, 1H, CH7); 1.76 (s, 15H, CH<sub>3</sub>Cp\*) ppm. <sup>13</sup>C NMR (125.75 MHz, CDCl<sub>3</sub>) δ 170.92 (C9); 152.9 (CH1); 145.3 (C3); 136.5 (C8a); 132.9 (CH6); 130.6 (C4a); 129.9 (CH7); 128.4 (CH5); 127.8 (CH8); 125.5 (CH4); 93.9 (d, <sup>1</sup>J(Rh,C) = 9 Hz, C<sub>Cp\*</sub>); 9.2 (CH<sub>3,Cp\*</sub>) ppm. Elemental analysis for C<sub>20</sub>H<sub>21</sub>ClNO<sub>2</sub>Rh·0.5H<sub>2</sub>O calc. C 52.82, H 4.88, N 3.08; found C 52.99, H 4.67, N 3.11

**Crystallographic structure determination:** Single crystals of complexes [RhCp\*(L)Cl] formed with 6-Mepic ( $1 \cdot \text{CH}_2\text{Cl}_2$ ) and 2-QA (**2**) were analyzed on a Bruker D8 Venture diffractometer equipped with multilayer monochromator, Mo K $\alpha$  INCOATEC micro focus sealed tube and Kryoflex II cooling device at 100 K. The single crystals were positioned at 35 mm from the detector and 2461 or 2076 frames for 2.4 or 8 s exposure time over  $0.4^\circ$  scan width were measured for complexes **1** and **2**, respectively. The structures were solved by direct methods and refined by full-matrix least-squares techniques. Non-hydrogen atoms were refined with anisotropic displacement parameters. Hydrogen atoms were inserted at calculated positions and refined with a riding model. The following computer programs were used: frame integration, Bruker SAINT software package [55] using a narrow-frame algorithm; absorption correction, SADABS [56]; structure solution, SHELXS-2013 [57]; refinement, SHELXL-2013 [57], OLEX2 [58], SHELXLE [59]; molecular diagrams, OLEX2 [58]. The crystallographic data files for the complexes have been deposited with the Cambridge Crystallographic Database as CCDC 1508154 ( $1 \cdot \text{CH}_2\text{Cl}_2$ ) and CCDC 1508153 (**2**). Crystal data and structure refinement details for complexes  $1 \cdot \text{CH}_2\text{Cl}_2$  and **2** are given in **Table S1**.

**pH-Potentiometric measurements:** pH-potentiometric measurements determining proton dissociation constants of ligands and overall stability constants for tested RhCp\* complexes were carried out in at  $25.0 \pm 0.1^\circ\text{C}$  in water and at a constant ionic strength of 0.20 M  $\text{KNO}_3$ . The titrations were performed in a carbonate-free KOH solution (0.20 M). The exact concentrations of  $\text{HNO}_3$  and KOH solutions were determined by pH-potentiometric titrations. An Orion 710A pH-meter equipped with a Metrohm “double junction” combined electrode (type 6.0255.100) and a Metrohm 665 Dosimat burette were used for the pH-potentiometric measurements. The electrode system was calibrated to the  $\text{pH} = -\log[\text{H}^+]$  scale by means of blank titrations (strong acid vs. strong base:  $\text{HNO}_3$  vs. KOH), as suggested by Irving *et al.* [60]. The average water ionization constant,  $\text{p}K_w$ , was determined as  $13.76 \pm 0.01$  at  $25.0^\circ\text{C}$ ,  $I = 0.20 \text{ M}$  ( $\text{KNO}_3$ ), which is in accordance to literature [61]. The pH-potentiometric titrations were performed in the pH range between 2.0 and 11.5. The initial volume of the samples was 10.0 mL. The ligand concentration was 1.0 mM and was investigated at metal ion-to-ligand ratios of 1:1, 1:1.5, and 1:2. The accepted fitting between the measured and calculated titration data points regarding the volume of the titrant was  $< 10 \mu\text{L}$ . Samples were degassed by bubbling purified argon through them for about 10 minutes prior to the measurements and the inert gas was also passed over the solutions during the titrations.

Calculations were performed with the computer program PSEQUAD [46] in the same way as in our previous works [27,28,32,33].

**UV-Vis spectrophotometric,  $^1\text{H}$  NMR titrations and determination of distribution coefficients:** A Hewlett Packard 8452A diode array spectrophotometer was used to record the UV-Vis spectra in the interval 200–800 nm. The path length ( $l$ ) was 0.1, 0.2, 0.5, 1, 2, or 4 cm. The overall stability constant of complex **3** (with 3-iQA) was determined spectrophotometrically by competition titrations using the complex in the presence of ethylenediamine at pH 7.40 (20 mM phosphate buffer) and at an ionic strength of 0.20 M ( $\text{KNO}_3$ ). Samples contained 99  $\mu\text{M}$   $[\text{RhCp}^*(\text{H}_2\text{O})_3]^{2+}$  and 99  $\mu\text{M}$  3-iQA, while the concentration of ethylenediamine was varied between 0–148  $\mu\text{M}$ . Absorbance data were recorded in a wavelength interval between 270 and 450 nm after 24 h of incubation. UV-Vis spectra were used to investigate the  $\text{H}_2\text{O}/\text{Cl}^-$  exchange processes of complexes at 250  $\mu\text{M}$  (**1**, **2**) or 100  $\mu\text{M}$  (**3**) concentration, at pH 7.40 (20 mM phosphate buffer) as a function of chloride concentrations (0–330 mM).

$D_{7.4}$  values of the  $[\text{RhCp}^*(\text{L})(\text{Z})]$  complexes **1–3** (where  $\text{Z} = \text{H}_2\text{O}/\text{Cl}^-$ ) and the ligands as well as the organorhodium  $\text{RhCp}^*$  fragment were determined by the traditional shake-flask method in *n*-octanol/buffered aqueous solution at pH 7.40 at various chloride concentrations using UV-Vis photometry as described in our former work [33,52].

$^1\text{H}$  NMR studies were carried out on a Bruker Ultrashield 500 Plus instrument. All  $^1\text{H}$  NMR spectra were recorded with the WATERGATE water suppression pulse scheme using DSS internal standard. Ligands 6-Mepic, 2-QA and 3-iQA were dissolved in a 10% (v/v)  $\text{D}_2\text{O}/\text{H}_2\text{O}$  mixture to yield a concentration of 1 or 2 mM and were titrated at 25 °C, at  $I = 0.20$  M ( $\text{KNO}_3$ ) in absence or presence of  $[\text{RhCp}^*(\text{H}_2\text{O})_3]^{2+}$  at 1:1 metal-to-ligand ratio. Stability constants for the complexes were calculated by the computer program PSEQUAD [46].

### **Cell lines, culture conditions and cytotoxicity tests in cancer cell lines**

**Cell lines and culture conditions:** CH1/PA-1 cells (identified via STR profiling as PA-1 ovarian teratocarcinoma cells by Multiplexion, Heidelberg, Germany) were a gift from Lloyd R. Kelland, CRC Center for Cancer Therapeutics, Institute of Cancer Research, Sutton, UK. SW480 (human adenocarcinoma of the colon), and A549 (human non-small cell lung cancer) cells were provided by Brigitte Marian (Institute of Cancer Research, Department of Medicine I, Medical University of Vienna, Austria). All cell culture reagents were obtained from Sigma-Aldrich and plasticware from Starlab (Germany). Cells were grown in 75  $\text{cm}^2$  culture flasks as adherent monolayer cultures in minimum essential medium (MEM) supplemented with 10% heat-inactivated fetal calf serum, 1 mM sodium pyruvate, 4 mM L-

glutamine, and 1% non-essential amino acids (from 100 × ready-to-use stock). Cultures were maintained at 37 °C in humidified atmosphere composed of 95% air and 5% CO<sub>2</sub>.

**MTT assay:** Cytotoxic effects were determined by means of a colorimetric microculture assay (MTT assay). For this purpose, cells were harvested from culture flasks by trypsinization and seeded in 100 µL/well aliquots into 96-well microculture plates. Cell densities of 1.0×10<sup>3</sup> cells/well (CH1/PA-1), 2.0×10<sup>3</sup> cells/well (SW480), and 3.0×10<sup>3</sup> cells/well (A549) were chosen in order to ensure exponential growth of untreated controls throughout the experiment. Cells were allowed to settle and resume exponential growth in drug-free complete culture medium for 24 h. Test compounds (**1** and **2**) were then dissolved in DMSO first, diluted in complete culture medium and added to the plates where the final DMSO content did not exceed 0.5%, whereas **3** was dissolved in pure complete culture medium. After 96 h of exposure, all media were replaced with 100 µL/well of a 1:7 MTT/RPMI 1640 solution (six parts of RPMI1640 medium supplemented with 10% heat-inactivated fetal bovine serum and 4 mM L-glutamine; one part of 5 mg/mL MTT reagent in phosphate-buffered saline (PBS)). After incubation for 4 h, the supernatants were removed and the formazan crystals formed by viable cells were dissolved in 150 µL DMSO per well. Optical densities at 550 nm were measured with a microplate reader (BioTek ELx808) using a reference wavelength of 690 nm to correct for unspecific absorption. The quantity of viable cells was expressed as percentage of untreated controls, and 50% inhibitory concentrations (IC<sub>50</sub>) were calculated from concentration-effect curves by interpolation. Evaluation is based on means from three independent experiments, each comprising three replicates per concentration level.

## Acknowledgements

This work was supported by the Hungarian National Research, Development and Innovation Office-NKFI through the projects PD103905, GINOP-2.3.2-15-2016-00038, the J. Bolyai Research Scholarship of the Hungarian Academy of Sciences (E.A.E.) and Austrian-Hungarian Scientific & Technological Cooperation TÉT\_15-1-2016-0024. The contribution of Ms. Klaudia Cseh to cytotoxicity tests is gratefully acknowledged.

## References

- [1] Y. Jung, S.J. Lippard, *Chem. Rev.* 107 (2007) 1387-1407.
- [2] G.N. Kaluderovic, R. Paschke, *Curr. Med. Chem.* 18 (2011) 4738-4752.
- [3] M.A. Jakupec, M. Galanski, V.B. Arion, C.G. Hartinger, B.K. Keppler, *Dalton Trans.* (2008) 183-194.
- [4] C.G. Hartinger, M.A. Jakupec, S. Zorbas-Seifried, M. Groessl, A. Egger, W. Berger, H. Zorbas, P.J. Dyson, B.K. Keppler, *Chem. Biodivers.* 5 (2008) 2140-2155.
- [5] R. Trondl, P. Heffeter, C.R. Kowol, M.A. Jakupec, W. Berger, B.K. Keppler, *Chem. Sci.* 5 (2014) 2925-2932.
- [6] A. Bergamo, G. Sava, *Chem. Soc. Rev.* 44 (2015) 8818-8835.
- [7] A.A. Nazarov, C.G. Hartinger, P.J. Dyson, *J. Organomet. Chem.* 751 (2014) 251-260.
- [8] A.F.A. Peacock, S. Parsons, P.J. Sadler, *J. Am. Chem. Soc.* 129 (2007) 3348-3357.
- [9] Y. Geldmacher, M. Oleszak, W.S. Sheldrick, *Inorg. Chim. Acta* 393 (2012) 84-102.
- [10] L. Dacsi, H. Elias, U. Frey, A. Hörnig, U. Koelle, A.E. Merbach, H. Paulus, J.S. Schneider, *Inorg. Chem.* 34 (1995) 306-315.
- [11] C.H. Leung, H.J. Zhong, D.S.H. Chan, D.L. Ma, *Coord. Chem. Rev.* 257 (2013) 1764-1776.
- [12] R. Pettinari, F. Marchetti, C. Pettinari, F. Condello, A. Petrini, R. Scopelliti, T. Riedel, P.J. Dyson, *Dalton Trans.* 44 (2015) 20523-20531.
- [13] A.J. Millett, A. Habtemariam, I. Romero-Canelón, G.J. Clarkson, P.J. Sadler, *Organometallics* 34 (2015) 2683-2694.
- [14] M.U. Raja, J. Tauchman, B. Therrien, G. Süss-Fink, T. Riedel, P.J. Dyson, *Inorg. Chim. Acta* 409 (2014) 479-483.
- [15] J. Markham, J. Liang, A. Levina, R. Mak, B. Johannessen, P. Kappen, C.J. Glover, B. Lai, S. Vogt, P.A. Lay, *Eur. J. Inorg. Chem.* 2017 (2017) 1812-1823.
- [16] A. Taylor, N. Carmichael, *Cancer Stud.* 2 (1953) 36-79.
- [17] M.J. Cleare, P.C. Hydes, *Met. Ions Biol. Syst.* 11 (1980) 1-62.
- [18] Y. Geldmacher, K. Splith, I. Kitanovic, H. Alborzina, S. Can, R. Rubbiani, M. A. Nazif, P. Wefelmeier, A. Prokop, I. Ott, S. Wölfl, I. Neundorf, W.S. Sheldrick, *J. Biol. Inorg. Chem.* 17 (2012) 631-646.
- [19] Y. Geldmacher, R. Rubbiani, P. Wefelmeier, A. Prokop, I. Ott, W.S. Sheldrick, *J. Organomet. Chem.* 696 (2011) 1023-1031.
- [20] M.A. Nazif, R. Rubbiani, H. Alborzina, I. Kitanovic, S. Wölfl, I. Ott, W.S. Sheldrick, *Dalton Trans.* 41 (2012) 5587-5598.
- [21] M.A. Scharwitz, I. Ott, Y. Geldmacher, R. Gust, W.S. Sheldrick, *J. Organomet. Chem.* 693 (2008) 2299-2309.
- [22] A.M. Angeles-Boza, H.T. Chifotides, J.D. Aguirre, A. Chouai, P.K.L. Fu, K.R. Dunbar, C. Turro, *J. Med. Chem.* 49 (2006) 6841-6847.
- [23] M. Kang, A. Chouai, H.T. Chifotides, K.R. Dunbar, *Angew. Chem. Int. Ed.* 45 (2006) 6148-6151.
- [24] Z. Li, A. David, B.A. Albani, J.P. Pellois, C. Turro, K.R. Dunbar, *J. Am. Chem. Soc.* 136 (2014) 17058-17070.
- [25] J.J. Soldevila-Barreda, I. Romero-Canelón, A. Habtemariam, P.J. Sadler, *Nat. Commun.* 6 (2015) article number: 6582.
- [26] J.J. Soldevila-Barreda, I. Romero-Canelón, A. Habtemariam, P.J. Sadler, *J. Inorg. Biochem.* 153 (2015) 322-333.
- [27] O. Dömötör, S. Aicher, M. Schmidlehner, M.S. Novak, A. Roller, M.A. Jakupec, W. Kandioller, C.G. Hartinger, B. K. Keppler, É.A. Enyedy, *J. Inorg. Biochem.* 134 (2014) 57-65.
- [28] É.A. Enyedy, O. Dömötör, C.M. Hackl, A. Roller, M.S. Novak, M.A. Jakupec, B.K. Keppler, W. Kandioller, *J. Coord. Chem.* 68 (2015) 1583-1601.
- [29] M.S. Eisen, A. Haskel, H. Chen, M.M. Olmstead, D.P. Smith, M.F. Maestre, R.H. Fish, *Organometallics* 14 (1995) 2806-2812.

- [30] S. Ogo, H. Chen, M.M. Olmstead, R.H. Fish, *Organometallics* 15 (1996) 2009-2013.
- [31] D.P. Smith, H. Chen, S. Ogo, A.I. Elduque, M. Eisenstein, M.M. Olmstead, R.H. Fish, *Organometallics* 33 (2014) 2389-2404
- [32] É.A. Enyedy, J.P. Mészáros, O. Dömötör, C.M. Hackl, A. Roller, B.K. Keppler, W. Kandioller, *J. Inorg. Biochem.* 152 (2015) 93-103.
- [33] O. Dömötör, V.F.S. Pape, N.V. May, G. Szakács, É.A. Enyedy, *Dalton Trans.* 46 (2017) 4382-4396.
- [34] Z. Liu, A. Habtemariam, A.M. Pizarro, S.A. Fletcher, A. Kisova, O. Vrana, L. Salassa, P.C.A. Bruijninx, G.J. Clarkson, V. Brabec, P.J. Sadler, *J. Med. Chem.* 54 (2011) 3011-3026.
- [35] A.F.A. Peacock, A. Habtemariam, S.A. Moggach, A. Prescimone, S. Parsons, P.J. Sadler, *Inorg. Chem.* 46 (2007) 4049-4059.
- [36] A. Habtemariam, M. Melchart, R. Fernandez, S. Parsons, I. D.H. Oswald, A. Parkin, F.P.A. Fabbiani, J.E. Davidson, A. Dawson, R.E. Aird, D.I. Jodrell, P.J. Sadler, *J. Med. Chem.* 49 (2006) 6858-6868.
- [37] E. Langner, K. Walczak, W. Jeleniewicz, W.A. Turski, G. Rajtar, *Eur. J. Pharmacol.* 757 (2015) 21-27.
- [38] I. Ivanovic, K.K. Jovanovic, N. Gligorijevic, S. Radulovic, V.B. Arion, K.S.A.M. Sheweshein, Z. Lj. Tesic, S. Grguric-Sipka, *J. Organomet. Chem.* 749 (2014) 343-349.
- [39] L. Booth, R.N. Haszeldine, M. Hill, *J. Chem. Soc. A* (1969) 1299-1303.
- [40] A.P. Abbott, G. Capper, D.L. Davies, J. Fawcett, D.R.J. Russell, *J. Chem. Soc. Dalton Trans.* (1995) 3709-3713.
- [41] É. Sija, C.G. Hartinger, B.K. Keppler, T. Kiss, É.A. Enyedy, *Polyhedron* 67 (2014) 51-58.
- [42] E. Lodyga-Chruscinska, G. Micera, E. Garribba, *Inorg. Chem.* 50 (2011) 883-899.
- [43] G. Anderegg, *Helv. Chim. Acta* 57 (1974) 1340-1346.
- [44] X. He, L. Long, X. Le, X. Chen, L. Ji, Z. Zhou, *Inorg. Chim. Acta* 285 (1999) 326-331.
- [45] A. Nutton, P.M. Baily, P.M. Maitlis, *J. Chem. Soc. Dalton Trans.* (1981) 1997-2002.
- [46] L. Zékány, I. Nagypál, in *Computational Methods for the Determination of Stability Constants* (Ed.: D.L. Leggett), Plenum Press, New York, 1985, pp. 291-353.
- [47] K.N. Raymond, C.J. Carrano, *Acc. Chem. Res.* 12 (1979) 183-190.
- [48] R.B. Martin, in *Cisplatin: Chemistry and Biochemistry of a Leading Anticancer Drug* (Ed.: B. Lippert), VCH & Wiley-VCH, Zürich, Switzerland, 1999, pp. 181-205.
- [49] M. Melchart, A. Habtemariam, O. Novakova, S. A. Moggach, F.P.A. Fabbiani, S. Parsons, V. Brabec, P.J. Sadler, *Inorg. Chem.* 46 (2007) 8950-8962.
- [50] F. Wang, H. Chen, S. Parsons, I.D.H. Oswald, J.E. Davidson, P.J. Sadler, *Chem. Eur. J.* 9 (2003) 5810-5820.
- [51] A.M. Pizarro, A. Habtemariam, P.J. Sadler, in *Medicinal Organometallic Chemistry (Topics in Organometallic Chemistry)*, 1<sup>st</sup> ed., vol. 32 (Eds.: G. Jaouen, N. Metzler-Nolte), Springer-Verlag, Heidelberg, Germany, 2010, pp. 21-56.
- [52] É.A. Enyedy, D. Hollender, T. Kiss, *J. Pharm. Biomed. Anal.* 54 (2011) 1073-1081.
- [53] I. Ivanovic, S. Grguric-Sipka, N. Gligorijevic, S. Radulovic, A. Roller, Z.L. Tesic, B.K. Keppler, *J. Serb. Chem. Soc.* 76 (2011) 53-61.
- [54] P. Gans, A. Sabatini, A. Vacca, *Talanta* 43 (1996) 1739-1753.
- [55] Bruker SAINT V8.32B Copyright © 2005-2015 Bruker AXS.
- [56] G.M. Sheldrick, SADABS, University of Göttingen, Germany, 1996.
- [57] G.M. Sheldrick, *Acta Cryst. A* 64 (2008) 112-122.
- [58] O.V. Dolomanov, L.J. Bourhis, R.J. Gildea, J.A.K. Howard, H. Puschmann, *J. Appl. Cryst.* 42 (2009) 339-341.
- [59] C.B. Hübschle, G.M. Sheldrick, B. Dittrich, *J. Appl. Cryst.* 44 (2011) 1281-1284.
- [60] H.M. Irving, M.G. Miles, L.D. Pettit, *Anal. Chim. Acta* 38 (1967) 475-488.
- [61] SCQuery, The IUPAC Stability Constants Database, Academic Software (Version 5.5), Royal Society of Chemistry, 1993-2005.